Cell Metabolism
Article

A Role for Brain-Specific Homeobox Factor Bsx in the Control of Hyperphagia and Locomotory Behavior

Maria Sakkou,[1] Petra Wiedmer,[2] Katrin Anlag,[1] Anne Hamm,[1] Eve Seuntjens,[1,4] Laurence Ettwiller,[1] Matthias H. Tschöp,[2,3] and Mathias Treier[1,*]
[1] Developmental Biology Unit, European Molecular Biology Laboratory, Meyerhofstrasse 1, 69117 Heidelberg, Germany
[2] German Institute of Human Nutrition, Potsdam-Rehbruecke, Department of Pharmacology, A.-Scheunert-Allee 114-116, 14558 Nuthetal, Germany
[3] Department of Psychiatry, University of Cincinnati, Obesity Research Centre - Genome Research Institute, 2170 E Galbraith Road, Cincinnati, OH 45237, USA
[4] Present address: Laboratory of Molecular Biology (Celgen), Department of Molecular and Developmental Genetics, K.U.Leuven, Gasthuisberg O&N1, Herestraat 49, 3000 Leuven, Belgium.
*Correspondence: treier@embl.de
DOI 10.1016/j.cmet.2007.05.007

SUMMARY

Food intake and activity-induced thermogenesis are important components of energy balance regulation. The molecular mechanism underlying the coordination of food intake with locomotory behavior to maintain energy homeostasis is unclear. We report that the brain-specific homeobox transcription factor Bsx is required for locomotory behavior, hyperphagia, and expression of the hypothalamic neuropeptides *Npy* and *Agrp*, which regulate feeding behavior and body weight. Mice lacking *Bsx* exhibit reduced locomotor activity and lower expression of *Npy* and *Agrp*. They also exhibit attenuated physiological responses to fasting, including reduced increase of *Npy/Agrp* expression, lack of food-seeking behavior, and reduced rebound hyperphagia. Furthermore, *Bsx* gene disruption rescues the obese phenotype of leptin-deficient *ob/ob* mice by reducing their hyperphagia without increasing their locomotor activity. Thus, Bsx represents an essential factor for NPY/AgRP neuronal function and locomotory behavior in the control of energy balance.

INTRODUCTION

Obesity is the result of positive energy balance, where caloric intake exceeds caloric expenditure over time. Since the brain plays a crucial role in the regulation of energy balance, a better understanding of the neuronal mechanisms required to maintain energy homeostasis is of outmost importance (Flier, 2004; Friedman, 2004; Morton et al., 2006; Schwartz and Porte, 2005).

The arcuate nucleus (ARC) of the hypothalamus harbors two distinct neuronal populations, which each receive multiple afferent signals conveying information about energy metabolism. "Orexigenic" neuropeptide Y / agouti-related peptide (NPY/AgRP) neurons promote weight gain, and they increase the secretion of other orexigenic neuropeptides including melanin-concentrating hormone (MCH) and hypocretin/orexin from the lateral hypothalamus. NPY/AgRP neurons are directly inhibited by leptin. In contrast, "anorexigenic" pro-opiomelanocortin (POMC) neurons inhibit food intake and promote weight loss in a leptin-dependent manner via α- and β-melanocyte stimulating hormones (α−MSH and β-MSH), products of POMC processing (Barsh and Schwartz, 2002; Lee et al., 2006). Many other satiety and hunger signals are sensed by these neurons, including ghrelin, insulin, glucose, and fatty acids (Badman and Flier, 2005). Both neuronal populations send dense projections to other neurons involved in energy metabolism located in the paraventricular nucleus (PVN), zona incerta, perifornical area and lateral hypothalamic area (Elias et al., 1998, 1999). NPY/AgRP neurons directly inhibit POMC neurons and antagonize the action of α−MSH on melanocortin-4 receptors (MC4R) via the release of AgRP (Cone, 2005).

Mutations that abolish the production of leptin, leptin receptor, MC4R or POMC lead to obesity in rodents and humans (Cone, 2005; Farooqi and O'Rahilly, 2005; Friedman and Halaas, 1998). Although intracerebroventricular administration of NPY or AgRP leads to a robust feeding response, decreased energy expenditure, and rapid weight gain in rodents (Hagan et al., 2000; Qian et al., 2002; Woods et al., 1998; Wortley et al., 2005), mutations that prevent the expression of NPY or AgRP have little effect on feeding behavior. However, loss of *Npy* does lead to the attenuation of the obesity syndrome of leptin-deficient *ob/ob* mice (Erickson et al., 1996b), and recent studies have firmly established that NPY/AgRP neurons are essential for feeding in adult mice since their ablation has reduced food intake to a much greater extent than deletion of either *Npy* or *Agrp* alone (Gropp et al., 2005;

Luquet et al., 2005), suggesting that NPY/AgRP neurons may harbor additional molecular players and functions important for body weight control.

Body weight remains stable when food intake and energy expenditure are in caloric balance. Energy expenditure can be partitioned into three major categories: basic cellular and physiological functions that require ATP (resting thermogenesis), the thermic effect of food, and thermogenesis induced by physical activity (Castaneda et al., 2005; Tou and Wade, 2002). Although physical activity expends calories, increased physical activity is essential for food acquisition. Thus, molecular mechanisms should exist that integrate these complex behaviors in the service of energy homeostasis. Consistent with that, both MCH and hypocretin/orexin are important in the control of locomotory behavior (Georgescu et al., 2005; Marsh et al., 2002; Thorpe and Kotz, 2005), and leptin signaling in the arcuate is necessary to maintain normal physical activity (Coppari et al., 2005).

We have found that the evolutionarily conserved brain-specific homeobox transcription factor Bsx is expressed in NPY/AgRP hypothalamic neurons, and that Bsx is required for normal *Npy*/*Agrp* expression, locomotory behavior, and the physiological response to food deprivation. Mice deficient for both Bsx and leptin have reduced body weight compared to leptin-deficient animals, and this is caused by attenuated hyperphagia paralleled by low *Npy*/*Agrp* expression. In contrast, *Bsx*-deficiency does not improve locomotor activity in leptin-deficient mice, revealing an extraordinary function of Bsx in the molecular regulation of feeding and locomotory behavior.

RESULTS

Downregulation of *Npy* and *Agrp* Arcuate Nucleus Expression in *Bsx* Mutant Mice

We identified the brain-specific homeobox transcription factor Bsx in a screen for novel transcriptional regulators in the hypothalamus. *Bsx* is expressed from e10.5 in the ventral diencephalon, an area that gives rise to the hypothalamus (Cremona et al., 2004). In the adult mouse brain, *Bsx* expression is restricted to the hypothalamus with prominent expression in the arcuate nucleus (Figure 1A), the dorsomedial hypothalamus (DMH), and scattered expression in the LHA (Figure S1 in the Supplemental Data available with this article online). Immunofluorescence staining of adult brain sections with Bsx antibodies faithfully recapitulated the *Bsx* expression pattern obtained by in situ hybridization (Figure 1B). Subsequent colocalization studies revealed that virtually all arcuate NPY/AgRP neurons express *Bsx* and that POMC neurons do not (Figures 1C–1F).

To assess the role of Bsx in murine development, we generated two different *Bsx* alleles, $Bsx^{\Delta HD}$ and $Bsx^{H2BeGFP}$, via homologous recombination in murine embryonic stem (ES) cells (Figures 2A–2F). Using the histone2BeGFP as a lineage marker, we could independently demonstrate the hypothalamic-specific expression of Bsx, consistent with the absence of detectable Bsx expression by RT-PCR in other brain regions (Figure S1). Taking advantage of both *Bsx* alleles, we established that loss of Bsx does not lead to a detectable loss of *Bsx*-expressing neurons, suggesting that the hypothalamic molecular neuroanatomy remained unchanged (Figures 2G–2I). This was further substantiated by normal expression patterns of hypothalamic neuropeptides (Figure S2). We next examined if loss of *Bsx* leads to a change of the gene expression program in NPY/AgRP neurons. In situ hybridization revealed a strong downregulation of *Npy* expression specifically in the arcuate in *Bsx* mutant mice (Figure 3A). Similarly, immunofluorescent staining for NPY revealed a significant reduction in the arcuate (Figure 3B). However, NPY staining in the PVN and other hypothalamic regions was still present, suggesting that

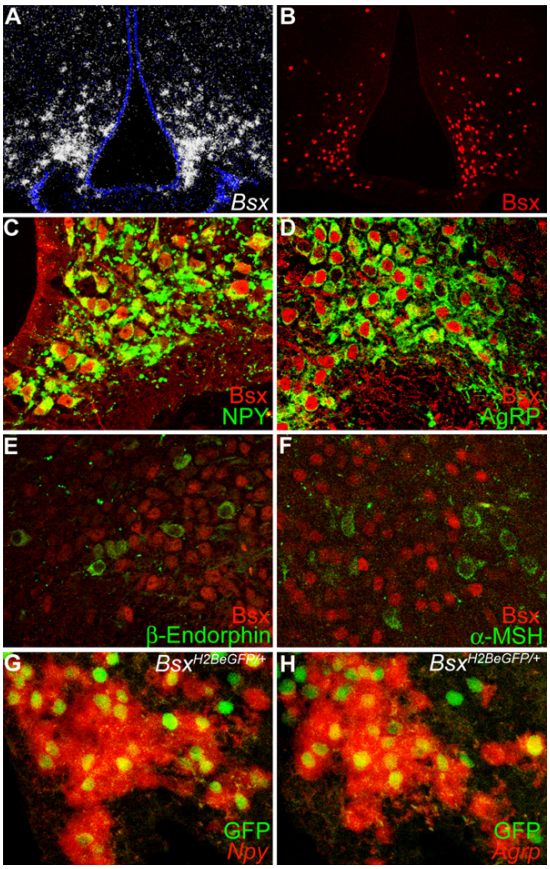

Figure 1. *Bsx* Expression Pattern in the Arcuate of Adult Mouse Brains

Arcuate *Bsx* expression in the adult mouse brain was visualized by (A) ^{35}S in situ hybridization with a *Bsx* probe and (B) immunohistochemistry with a rabbit Bsx antibody. Single-layer confocal images of double immunofluorescence stainings on coronal brain sections from colchicine-treated 9-week-old wild-type mice with (C) Bsx and NPY, (D) Bsx and AgRP, (E) Bsx and β-endorphin, and (F) Bsx and α-MSH antibodies detects *Bsx* expression in NPY/AgRP neurons. Single-layer confocal projections of double in situ/immunofluorescence analysis of (G) *Npy* mRNA or (H) *Agrp* mRNA and GFP protein on coronal brain sections from 9-week-old heterozygote $Bsx^{H2BeGFP/+}$ mice.

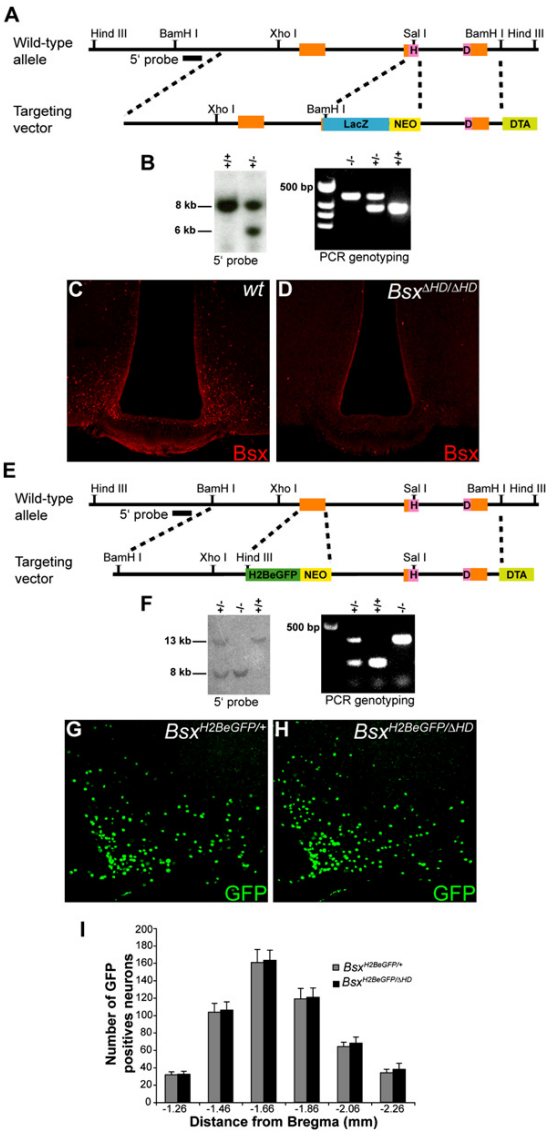

Figure 2. Generation of *Bsx*$^{\Delta HD}$ and *Bsx*^{H2BeGFP} Alleles

(A) *Bsx*$^{\Delta HD}$ allele was generated fusing the lacZ coding sequence in frame with the *Bsx* open reading frame deleting at the same time part of exon2 which encodes helix 1+2 of the homeodomain.

(B) Genomic DNA was digested with BamHI and probed with a 5′ outside probe to detect homologous recombination in embryonic stem cells. PCR analysis was subsequently used for genotyping.

(C and D) Bsx immunostaining on coronal brain sections at the level of the hypothalamus from a 9-week-old wild-type and *Bsx*$^{\Delta HD/\Delta HD}$ mouse with a rat Bsx antibody, respectively.

(E) *Bsx*^{H2BeGFP} allele was generated replacing exon1 of *Bsx* starting at the ATG with a sequence coding for Histone2BeGFP.

(F) Southern blot analysis of tail DNA digested with HindIII and probed with a 5′ outside probe to detect homologous recombination. PCR analysis was subsequently used for genotyping.

(G and H) GFP emission from coronal brain sections of 9-week-old *Bsx*$^{H2BeGFP/+}$ and mutant *Bsx*$^{H2BeGFP/\Delta HD}$ mice at the level of the arcuate, demonstrating that number of *Bsx*-expressing neurons within the hypothalamus are not changed.

(I) Counting of GFP-positive nuclei between heterozygote *Bsx*$^{H2BeGFP/+}$ and mutant *Bsx*$^{H2BeGFP/\Delta HD}$ in the brain sections reveals no difference in the number of *Bsx*-expressing cells in the arcuate.

projection of NPY-expressing neurons was not altered (Figure 3B and data not shown). Expression of *Agrp* was also downregulated in *Bsx* mutant brains (Figure 3C). We independently confirmed these results by quantitative RT-PCR which revealed a 5-fold downregulation for hypothalamic *Npy* and *Agrp* expression in *Bsx* mutant animals, respectively (Figures 3F and 3G). In contrast, but consistent with our immunohistochemical colocalization results, expression of *Pomc* and *Cocaine-amphetamine regulated transcript* (*Cart*) was unchanged (Figures 3D, 3E, 3H, and 3I).

Bsx Mutant Mice Display Altered Locomotory Behavior

The substantial decrease in *Npy* and *Agrp* expression in *Bsx* mutant brains prompted us to condust a more detailed analysis of the metabolic status of *Bsx* mutant animals. Although body weight of *Bsx* mutant animals did not differ from that of their wild-type littermates (Figures 4A–4C), they had a significant increase in fat mass (Figure 4D). There was no obvious change in energy expenditure, and slight decrease in the respiratory quotient (Figures 4E and 4F). Despite the massive downregulation of *Npy* and *Agrp* expression in *Bsx* mutant mice, the modest change in physiological parameters is consistent with the modest phenotype observed in *Npy* and *Agrp* knockout animals (Qian et al., 2002). Unlike what occurs in *Npy* or *Agrp*-deficient mice (Segal-Lieberman et al., 2003b; Wortley et al., 2005), locomotor activity of *Bsx* mutant mice was severely reduced (Figures 4I and 4J). In addition, a significant difference in body temperature was observed during the 12 hr period of darkness between *Bsx* mutant mice and their wild-type littermates (Figures 4G and 4H). These defects in *Bsx* mutant animals cannot therefore be explained by a downregulation of *Npy* or *Agrp*. The expression levels of other neuropeptides including MCH or orexin that are implicated in both feeding and locomotory behavior were not changed in *Bsx* mutant mice (Figure S2). *Bsx* mutant mice were similar to control littermates with respect to grip strength and performance on a rotarod, suggesting that motor coordination was not affected (data not shown).

Bsx mutant mice therefore have downregulated *Npy* and *Agrp* expression, which should reduce food consumption and increase energy expenditure leading to a lean phenotype, as well as reduced locomotion, which should decrease energy expenditure and promote body weight gain. The observed increase in fat mass suggests therefore that reduced motor activity induced thermogenesis is the prevailing of the two metabolic defects on normal chow.

Fasting Response Is Blunted in *Bsx* Mutant Mice

Expression of *Npy* and *Agrp* is strongly induced when mice are fasted (Hahn et al., 1998). To determine whether

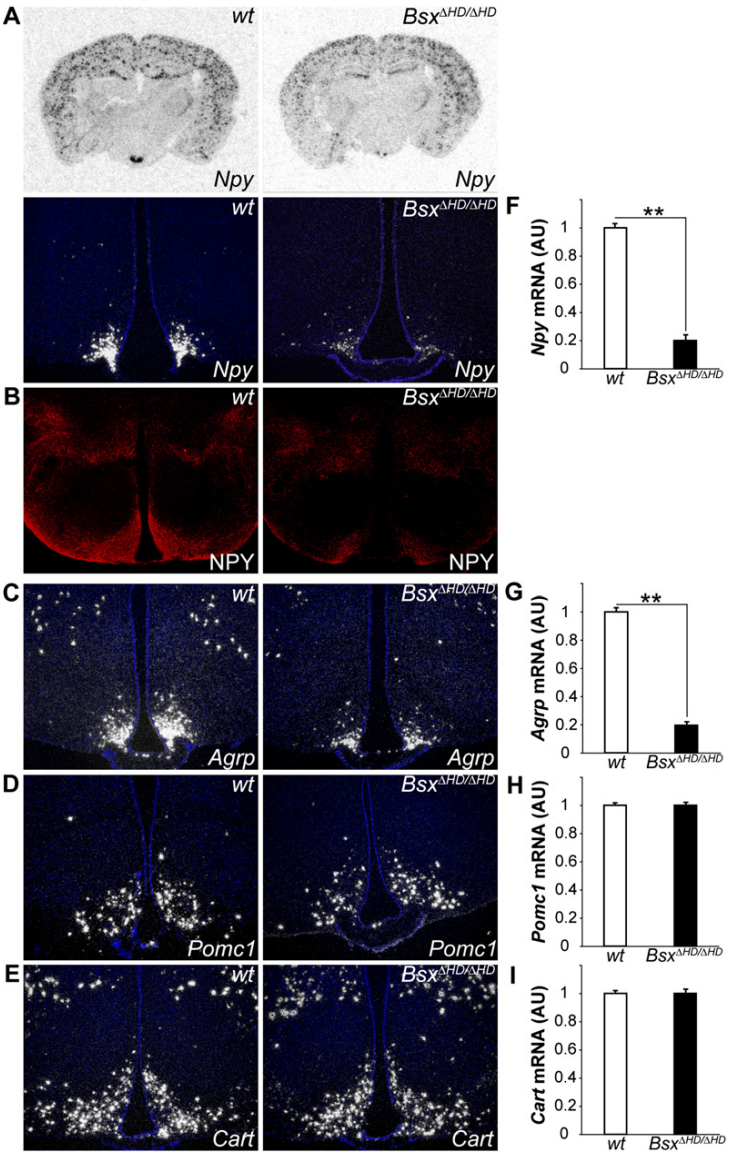

Figure 3. Downregulation of *Npy* and *Agrp* Expression in *Bsx* Mutant Mice

(A) ^{35}S in situ hybridization demonstrates downregulation of *Npy* expression specifically in the arcuate of *Bsx* mutant brains. (B) NPY levels are consistent with (A), also reduced. However the overall NPY staining pattern remains unchanged. Detection and comparison of (C) *Agrp*, (D) *Pomc1*, and (E) *Cart* expression levels by ^{35}S in situ hybridization between wild-type and *Bsx*$^{\Delta HD/\Delta HD}$ mice. Slides hybridized with all four probes were exposed to emulsion for 21 days. (F–I) Quantitative real-time PCR for (F) *Npy* and (G) *Agrp* shows a 5-fold downregulation of both transcripts in *Bsx* mutant mice, respectively (**$p < 0.05$). In contrast (H) *Pomc* and (I) *Cart* levels remained unchanged. AU, arbitrary units.

this induction requires Bsx, *Npy* and *Agrp* expression determined by ^{35}S in situ hybridization (Figures 5A–5H) and qRT-PCR (Figures 5I and 5J) was analyzed in wild-type and *Bsx* mutant mice after fasting. A robust increase in *Npy* and *Agrp* expression was seen in fasted control animals (Figures 5B–5F), whereas the absolute levels of *Npy* and *Agrp* in fasted *Bsx* mutant animals stayed below the levels of the nonfasted wild-type controls (compare Figure 5A with Figure 5D and Figure 5E with Figure 5H). Nonetheless, a reproducible small induction in *Npy* and *Agrp* expression was seen when nonfasted and fasted *Bsx* mutant animals were compared (compare Figure 5C with Figure 5D and Figure 5G with Figure 5H). These results imply an important, but not exclusive, role for Bsx in fasting-induced increase of *Npy* and *Agrp* gene expression. The low level of fasting-induced *Npy*/*Agrp* expression prompted us to assess food intake after fasting ("rebound feeding"). *Bsx* mutant animals ingested 40% less food than their comparably fasted wild-type littermates, consistent with the low levels of *Npy*/*Agrp* expression (Figure 5K). These data are in contrast to what has been observed in mice lacking *Npy* and/or *Agrp,* which do not show reduced rebound feeding (Erickson et al., 1996a; Qian et al., 2002; Sindelar et al., 2005). One explanation may be that the low expression of *Npy* and *Agrp* still observed in the *Bsx* mutant mice prevents a network-based compensatory mechanism as demonstrated in the case of *Npy*-deficiency (Luquet et al., 2005). Fasting also increases total dark- and light-phase locomotor activity in mice (Overton and Williams, 2004; Williams et al., 2003).

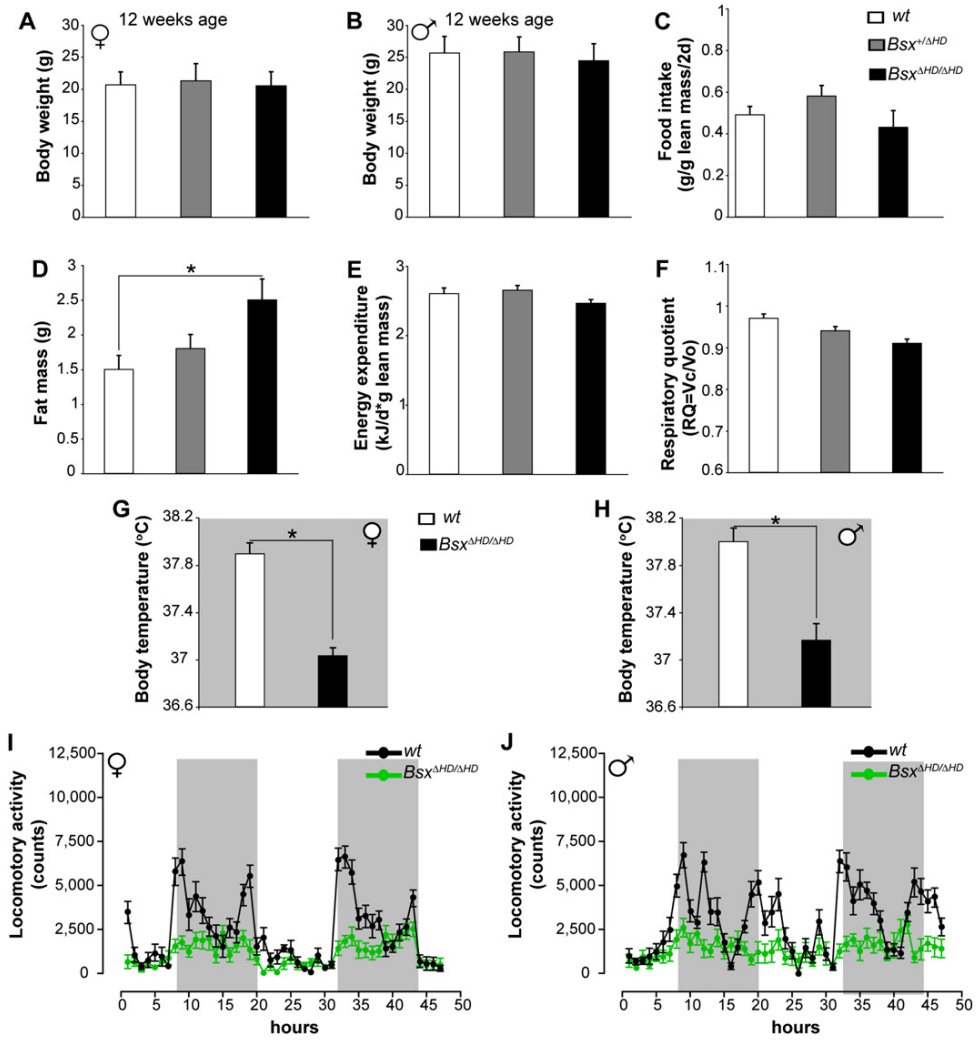

Figure 4. Reduced Locomotor Activity in *Bsx* Mutant Mice

(A and B) Average body weight of wild-type (WT), heterozygote, and homozygote female and male mice at the age of 12 weeks old; n = 12 for each genotype, values are the mean ± SEM.

(C) Average food consumption, determined by measuring 2 day food intake in mice.

(D) Adiposity of the mice was determined by measurements of the fat mass.

(E) Energy expenditure was measured over 2 days and averaged.

(F) Mean respiratory quotient was calculated as the ratio of Vco_2 produced/Vo_2 consumed over 2 days and averaged. For all the measurements, n = 12 for each genotype both sexes; values represent mean ± SEM, (*$p < 0.01$). In male and female mice, the tendencies in the three genotypes are the same for all the measurements, therefore data obtained from female mice are presented.

(G and H) Body core temperature during 12 hr period of darkness as measured by telemetry over a period of 2 days; n > 6 for each genotype, values are means ± SEM, (*$p < 0.01$).

(I and J) 48 hr locomotor activity traces determined as number of counts for both male and female mice n = 12 for each genotype and sex. Gray area represents dark period in (G)–(J).

Likewise, *Bsx* mutant animals did not significantly increase their home cage activity upon food deprivation, while their wild-type littermates did (Figures 5L and 5M). These data further demonstrate the simultaneous dependency on Bsx function in the behavioral responses to fasting.

The observation that *Bsx* gene expression itself increases in fasted wild-type mice and in leptin-deficient *ob/ob* mice points to another level of regulation for *Npy* and *Agrp* expression (Figure S3). In this respect, it is also interesting that a highly evolutionarily conserved Stat3 binding site is located in close proximity downstream of the *Bsx* gene (L.E. and M.T., unpublished data).

Ghrelin, a gut-derived peptide hormone whose circulating levels increase during fasting, is the only circulating

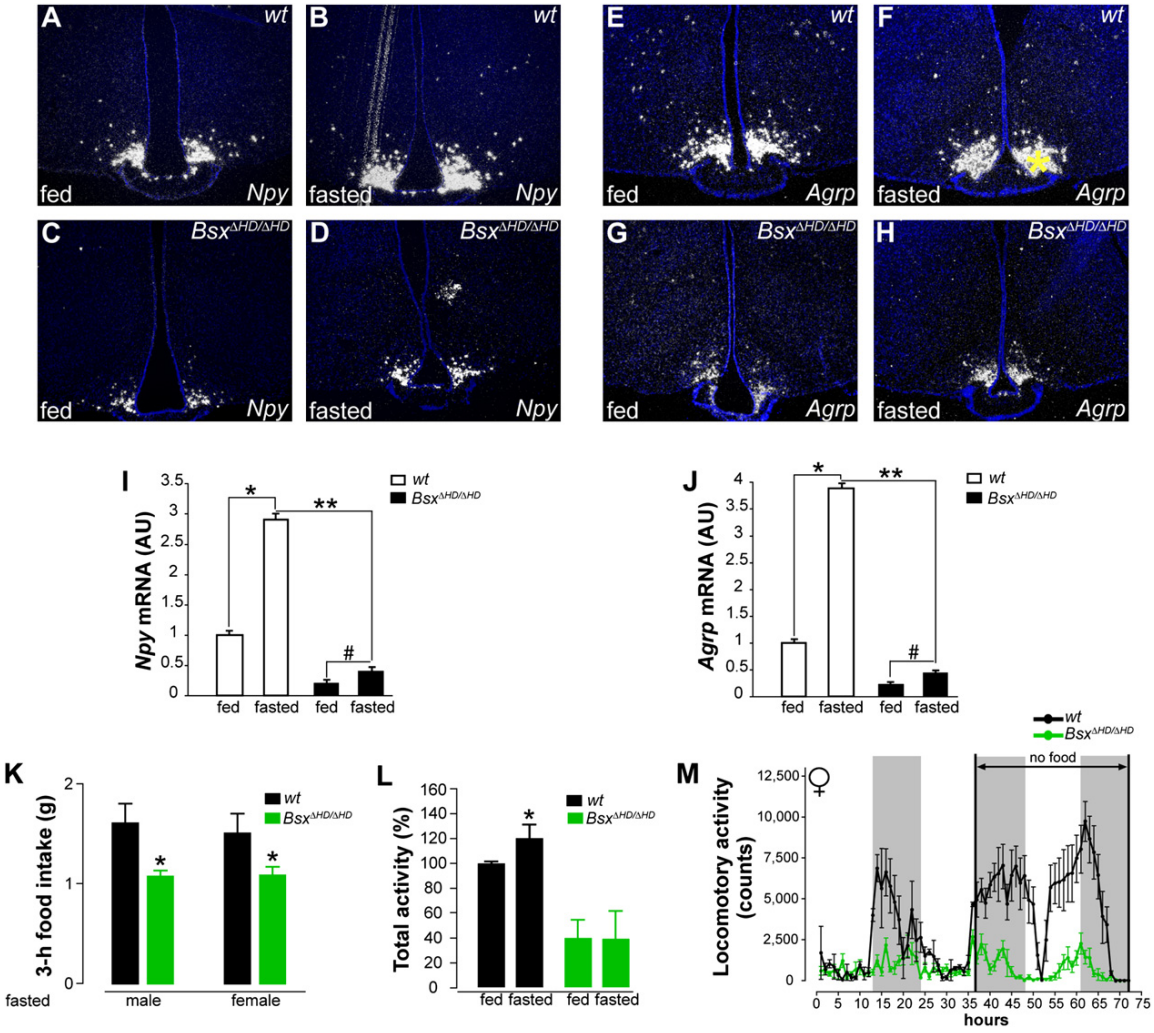

Figure 5. Bsx Is Required for Fasting-Induced Activation of *Npy/Agrp* Expression

(A–D) *Npy* ^{35}S in situ expression analysis in nonfasted and 48 hr fasted control and *Bsx* mutant mice (I) quantification by real-time PCR revealed a 7-fold higher expression of *Npy* in fasted control compared to *Bsx* mutant mice (**p < 0.05) and only a 2-fold ($^{\#}$p < 0.05) compared to 3-fold (*p < 0.05) induction of *Npy* expression comparing *Bsx* mutant mice with control littermates. (E–H) *Agrp* ^{35}S in situ expression analysis in nonfasted and 48 hr fasted control and *Bsx* mutant mice (J) quantification by real-time PCR revealed a 8-fold higher expression of *Agrp* in fasted control compared to *Bsx* mutant mice (**p < 0.05) and only a 2-fold ($^{\#}$p < 0.05) compared to 4-fold (*p < 0.05) induction of *Agrp* expression comparing *Bsx* mutant with control littermates. Slides hybridized with *Npy* and *Agrp* probes were exposed for 12 days. Asterisk in (F) marks overexposed and hence black region due to high-level *Agrp* expression. (K) 3 hr food intake in control and *Bsx* mutant male and female mice after 36 hr fasting (rebound refeeding). (L) 24 hr total activity was significantly increased in both sexes of wild-type but not *Bsx* mutant mice as compared to baseline levels (*p < 0.05). (M) both sexes of wild-type but not *Bsx* mutant animals show strong light phase activity during fasting (locomotor traces are shown only for females).

factor that directly stimulates NPY/AgRP neurons (Cowley et al., 2003; Hewson and Dickson, 2000; Tschop et al., 2000). It has been shown that the orexigenic action of peripheral ghrelin is mediated by NPY and AgRP (Chen et al., 2004). Consistent with the blunted fasting response in *Bsx* mutant animals food intake upon ghrelin administration was significantly lower in *Bsx* mutant mice compared to control littermates, although the ghrelin receptor, (*growth hormone secretagogue receptor*, *Ghsr),* is expressed normally in *Bsx*-deficient NPY/AgRP neurons (Figure S4).

Loss of *Bsx* Attenuates the Obesity Syndrome of *ob/ob* Mice

Similar to food-deprived animals, *ob/ob* mice lacking leptin have highly elevated *Npy* and *Agrp* expression in the arcuate. To explore the relationship between leptin signaling and Bsx function, we generated mice mutant for both *leptin* and *Bsx*. Double homozygous mutant *Bsx*$^{\Delta HD/\Delta HD}$*; ob/ob* mice were considerably leaner than their *ob/ob* littermates due to a reduction of fat mass (Figures 6A and 6H). In situ hybridization and qRT-PCR analysis revealed

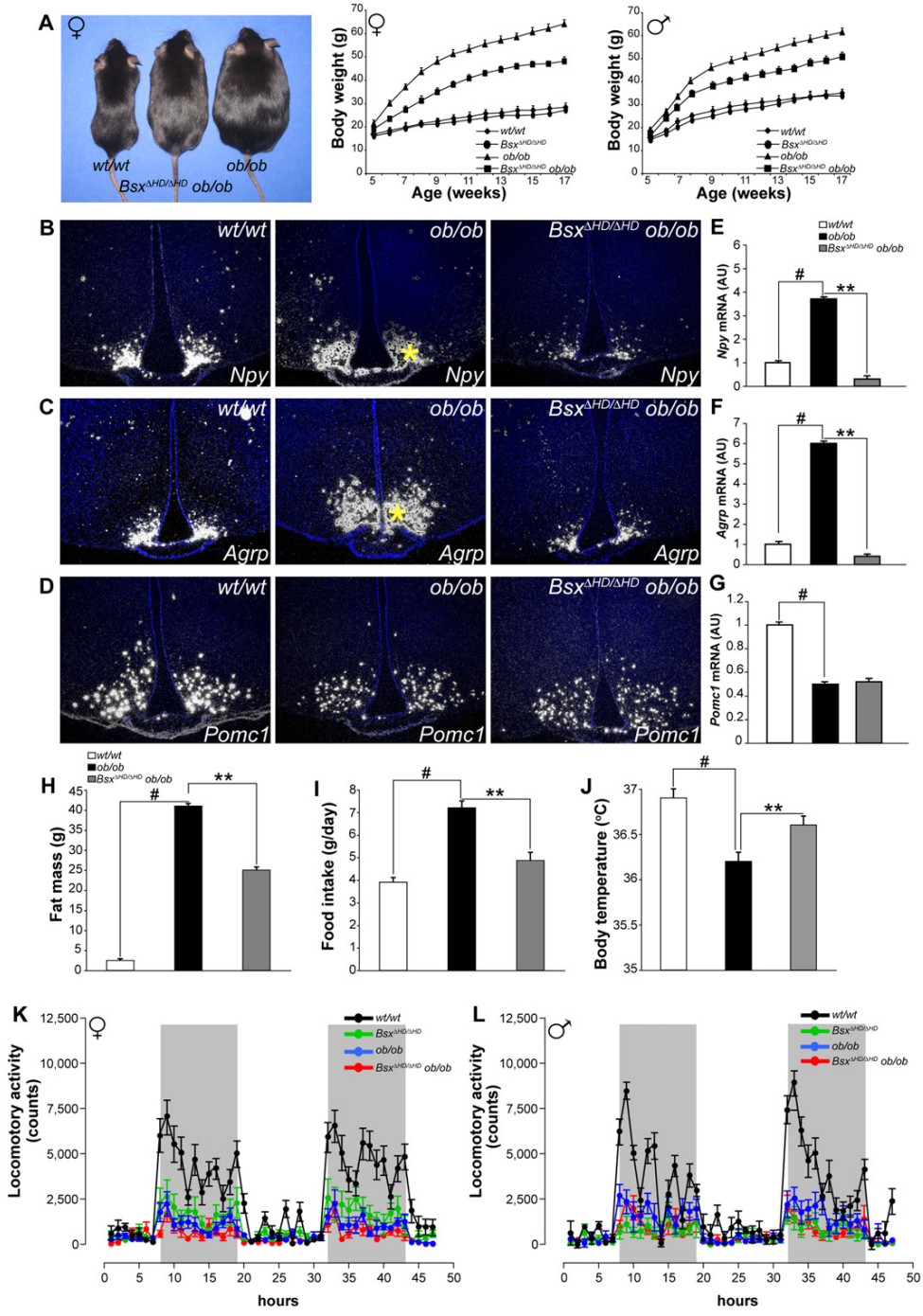

Figure 6. Attenuation of the Obesity Syndrome of *ob/ob* Mice by the Loss of *Bsx*

(A) Physical appearance (picture shows female mice) of control, $Bsx^{\Delta HD/\Delta HD}$*ob/ob*, and *ob/ob* mice, and body weight of female and male mice at various ages (A); n = 12 for each genotype; values are the means ± SEM.

(B–D) ^{35}S in situ hybridization for *Npy*, *Agrp* and *Pomc1* on brain coronal sections from control, *ob/ob*, and compound mutants $Bsx^{\Delta HD/\Delta HD}$*ob/ob*. The slides hybridized with *Npy, Agrp*, and *Pomc1* were exposed 21 days. Asterisks in (B) and (C) mark the overexposed and hence black region due to high levels of *Npy* and *Agrp* expression.

(E–G) quantitative real-time PCR shows a more than 3-fold difference in *Npy* ($^{\#}p < 0.05$) and a 6-fold difference in *Agrp* expression ($^{\#}p < 0.05$) between *ob/ob* and control mice and a 19-fold difference in *Npy* ($^{**}p < 0.05$) and a 28-fold difference in *Agrp* expression ($^{**}p < 0.05$) between *ob/ob* and $Bsx^{\Delta HD/\Delta HD}$*ob/ob* mice, whereas *Pomc1* expression levels remained unchanged.

that expression of *Npy* and *Agrp* did not exceed the low levels observed in *Bsx* mutant animals and were not increased as observed in *ob/ob* animals (compare Figures 6B, 6C, 6E, and 6F with Figures 3A, 3C, 3F, and 3G). No difference was detected in *Pomc* expression between *ob/ob* and $Bsx^{\Delta HD/\Delta HD}$;*ob/ob* mice, which was lower than in wild-type controls in both cases (Figure 6D and 6G). Consistent with the downregulation of *Npy* expression in $Bsx^{\Delta HD/\Delta HD}$;*ob/ob* mice, food intake was increased by only 20% compared to control littermates, whereas *ob/ob* mice ingested 70% more food (Figure 6I). Thus, $Bsx^{\Delta HD/\Delta HD}$;*ob/ob* mice have a considerably reduced hyperphagia (~60%). Body temperature in $Bsx^{\Delta HD/\Delta HD}$;*ob/ob* mice was elevated compared to that of *ob/ob* mice, which may reflect a partial rescue of impaired resting thermogenesis (Figure 6J).

Since glucose homeostasis and glycemic control are improved in *ob/ob* mice which are also deficient for *Npy* (*ob/ob*;$Npy^{-/-}$) (Erickson et al., 1996b), we measured these parameters in the $Bsx^{\Delta HD/\Delta HD}$;*ob/ob* animals. Loss of *Bsx* significantly ameliorated the hyperglycemia and hyperinsulinemia observed in *ob/ob* animals. Fertility of *ob/ob* females was also improved by removal of Bsx, similar to what had been observed for *ob/ob*;$Npy^{-/-}$ mice (Table S1). Despite the significant weight reduction in $Bsx^{\Delta HD/\Delta HD}$;*ob/ob* mice, locomotor activity levels were not higher compared to *ob/ob* mice (Figures 6K and 6L). This result implies that Bsx function is an essential genetic component and independent determinant in the hypothalamic regulation of locomotory behavior.

Bsx Occupies *Npy* and *Agrp* Regulatory Sequence Elements In Vivo

The low expression of *Npy* and *Agrp* after fasting in *Bsx* deficient mice and in $Bsx^{\Delta HD/\Delta HD}$;*ob/ob* double-mutant mice suggested that Bsx may directly regulate *Npy* and *Agrp* expression. Rat PC12 cells, which express *Npy* at low levels (Higuchi et al., 1988), do not express endogenous *Bsx* (data not shown). We therefore hypothesized that expression of *Bsx* in PC12 cells would stimulate *Npy* expression. Quantitative RT-PCR revealed a 50-fold induction of *Npy* in cells transfected to express Bsx over the signal that was detected in mock-transfected cells (Figure 7A). To see if this induction is specific to Bsx or if other homeobox transcription factors could produce similar effects, we used the closely related homeobox gene Nkx2.1/TTF-1, which is coexpressed during development in the hypothalamus, as a control. Overexpression of Nkx2.1 or another control, Pit-1, led to only a modest increase in *Npy* RNA of 4- or 2-fold, respectively (Figure 7A). Activation of *Npy* expression can also be mimicked by treating PC12 cells with the cAMP analog DibcAMP and further stimulated with PMA (Higuchi et al., 1988), consistent with reports implicating the transcription factor CREB in *Npy* regulation during starvation (Shimizu-Albergine et al., 2001). We repeated this experiment in PC12 cells and found that *Npy* expression was activated about the same level by DibcAMP/PMA treatment as in the *Bsx* transfection experiment. Unexpectedly, when we stimulated *Bsx*-transfected PC12 cells with DibcAMP/PMA, we observed a synergistic increase in *Npy* expression (Figure 7A). Using reciprocal GST pull-down experiments, we found that Bsx and CREB physically interact (Figure 7E). To identify the regulatory sequences to which CREB and Bsx bind in the *Npy* promoter region we took a bioinformatic comparative sequence analysis approach. Aligning various mammalian species only one region approximately 50kb upstream of the *Npy* gene start site could be identified that is conserved and contained a conserved CREB and homeobox binding site next to each other (Figures 7B and S5). When we tested this DNA fragment in front of a basal promoter driving luciferase we could recapitulate the synergistic activation seen in PC12 cells of the *Npy* gene by Bsx and cAMP (Figure 7C). Furthermore, chromatin immunprecipitation (ChIP) using a Bsx-specific antibody on H2BeGFP-positive cells sorted from heterozygote and *Bsx* mutant animals demonstrated occupancy of the predicted homeobox binding site by Bsx in vivo (Figure 7D).

Analogously, it has been reported that FoxO1 translocates to the nucleus during fasting where it stimulates *Agrp* gene expression (Kitamura et al., 2006). This can be mimicked using a constitutive FoxO1-ADA expression vector. We therefore transfected AtT20 cells with combinations of *Bsx* and *FoxO1* expression vectors and found that Bsx and FoxO1 cooperate to induce *Agrp* expression (Figure 7G). Close to the reported FoxO1 and Stat3 binding sites there are two highly conserved homeobox binding sites in mammals (C.B. Kaelin and G.S. Barsh, personal communication) (Figure 7H). Employing a similar approach as for the *Npy* element we could demonstrate that these sites are occupied by Bsx in vivo and are able to act in concert with the neighboring FoxO1 site in *Agrp* gene induction (Figures 7I and 7J). Furthermore, using GST pull-down experiments, we also found that Bsx and FoxO1 physically interact (Figure 7K). These results together indicate that Bsx can directly stimulate *Npy* and *Agrp* expression and is able to physically interact with the two transcription factors CREB and FoxO1 that have been implicated in the fasting dependent up-regulation of these neuropeptides.

DISCUSSION

Hypothalamic neurons producing NPY and AgRP have recently been confirmed as essential centers of food intake

(H) Adiposity was determined by fat mass measurements of mice from each genotype at 16 weeks of age; values represent means ±SEM, ($^{*}p < 0.01$, $^{\#}p < 0.01$).
(I) Food intake was determined by monitoring of food intake over 2 days; n > 9 for each genotype, values are the means ± SEM, ($^{*}p < 0.01$, $^{\#}p < 0.01$).
(J) Body core temperature as measured by telemetry over a period of 2 days; n > 9 for each genotype, values are means ± SEM, ($^{*}p < 0.01$, $^{\#}p < 0.01$).
(K and L) 48 hr locomotor activity traces for male and female mice of the indicated genotypes; n = 6 for every genotype.

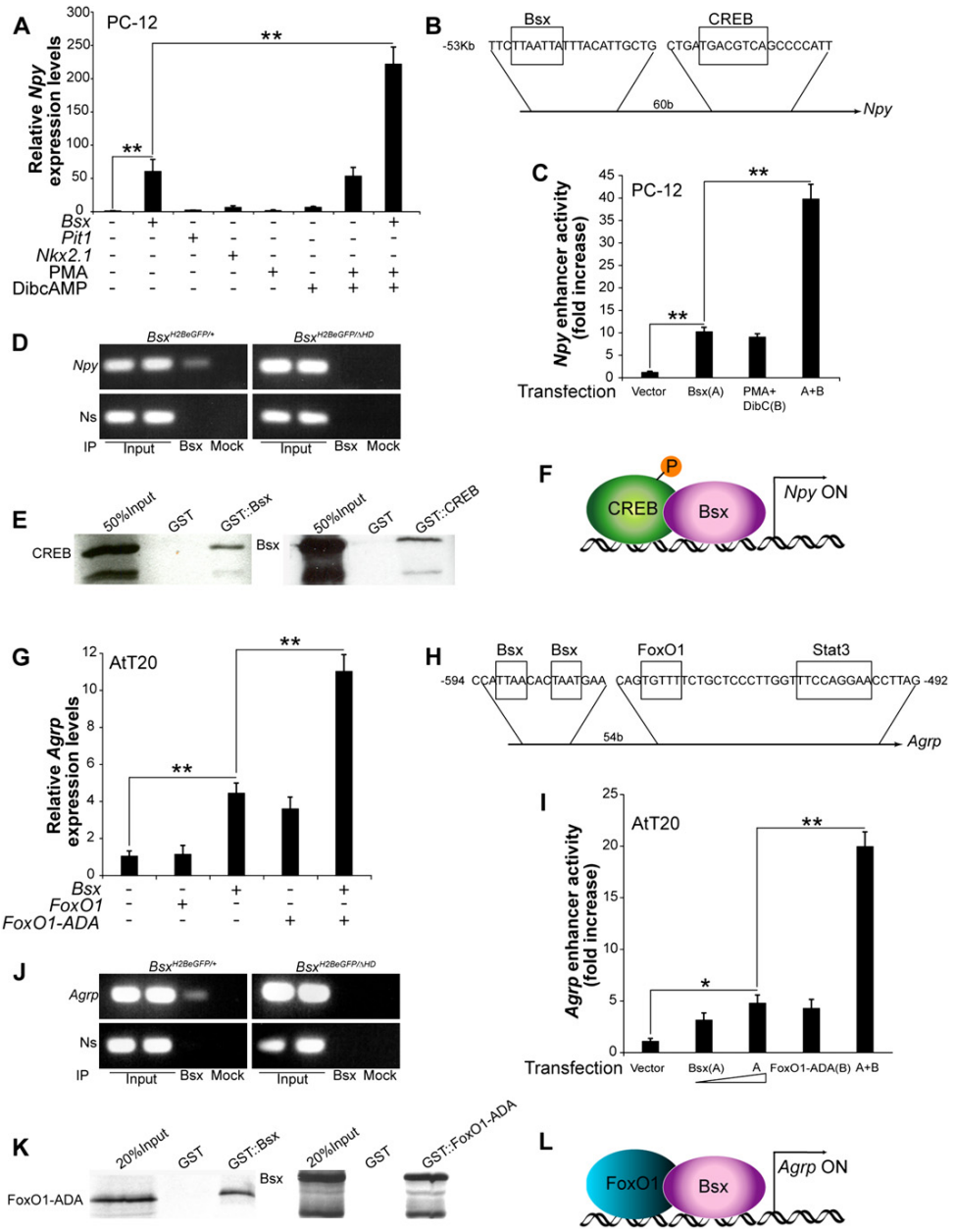

Figure 7. Regulation of *Npy* and *Agrp* Gene Expression by Bsx

(A) *Npy* expression analysis using quantitative RT-PCR from PC-12 cells transiently transfected with *Bsx*, *Pit1*, and *Nkx2.1* expression vectors and/or treated with PMA and/or DibcAMP; data were normalized for TBP (**$p < 0.01$).

(B) Sequence of the *Npy* regulatory element containing the conserved Bsx and CREB binding sites.

(C) Activation of a heterologous promoter driven by the *Npy* regulatory element in PC12 cells.

(D) Chromatin immunoprecipitation using a Bsx specific antibody shows occupancy of Bsx on the predicted binding site in isolated H2BeGFP labeled hypothalamic cells from heterozygous but not *Bsx* mutant mice.

(E) GST pull-down interaction assay with GST::Bsx and in vitro translated full length CREB protein, and GST::CREB with in vitro translated Bsx protein.

(F) Model of *Npy* gene regulation.

(G) *Agrp* expression analysis using quantitative RT-PCR from AtT20 cells transiently transfected with *Bsx* and *FoxO1* expression vectors; data were normalized for 18S (**$p < 0.01$).

(H) Sequence of the *Agrp* regulatory element containing the conserved Bsx, FoxO1, and Stat3 binding sites.

(I) Activation of a heterologous promoter driven by the *Agrp* regulatory element in AtT20 cells.

and body weight regulation (Gropp et al., 2005; Luquet et al., 2005). The most powerful signals known to activate these arcuate neurons are food deprivation or administration of ghrelin (Cowley et al., 2003; Hahn et al., 1998). The present data indicate that the brain-specific homeobox transcription factor Bsx is required for adaptive increases in *Npy* and *Agrp* expression, ghrelin stimulated food intake, and for a normal hyperphagic response to fasting. Since deficiency for *Bsx* also rescues the hyperphagia of leptin-deficient mice similar to what has been observed in *ob*/*ob* mice with *Npy* deficiency (Erickson et al., 1996b), we conclude that Bsx may also be required for nonphysiological types of hyperphagia. However, *Bsx* mutant mice in addition show a reduction in *Agrp* expression. As AgRP plays a well-known function in melanocortin signaling (Cone, 2005), it may be interesting to see if *Bsx* deficiency also ameliorates the obesity phenotype of melanocortin-4 receptor mice which is in part caused by hyperphagia (Huszar et al., 1997). Interestingly, MC4R mutant mice do show de novo expression of *Npy* in the DMH region where *Bsx* expression is also observed (Kesterson et al., 1997).

Despite the central importance of the two orexigenic peptides NPY and AgRP for food intake and energy metabolism their signal-dependent transcriptional regulation is still not fully understood. In case of *Agrp* gene regulation, elegant genetic experiments have shown that leptin receptor-dependent Stat3-signaling is modulating *Agrp* expression (Bates et al., 2003). More recent in vivo studies have confirmed an essential role for *cis*-acting Stat3 binding sites in the regulation of *Agrp,* but also proposed a requirement for additional factors (Kaelin et al., 2006). Indeed, subsequent work has shown that FoxO1, the distal effector of insulin signaling, activates *Agrp* expression and that leptin signaling through Stat3 can inhibit FoxO1 function by a transcriptional squelching mechanism (Kitamura et al., 2006). In contrast, the transcriptional regulation of *Npy* gene expression in vivo is less clear than for *Agrp*. In particular, the demonstrated inhibition of *Npy* gene expression by leptin, which requires PI3K signaling, is not well understood at the transcriptional level (Morrison et al., 2005; Xu et al., 2005). The identification of an evolutionary conserved regulatory *cis*-acting element approximately 50 kb upstream of the *Npy* transcriptional start site which is bound by *Bsx* in vivo will now allow similar in vivo studies as mentioned above for *Agrp*. Our study thus adds Bsx to the transcriptional network required for *Agrp* and *Npy* gene expression. The highly restricted Bsx expression pattern provides tissue specificity that may work in the context of more generally required transcriptional regulators such as CREB, Stat3 and FoxO1. This situation resembles the roles of other homeodomain transcription factors in other organ systems (Scully and Rosenfeld, 2002).

The phenotypic analysis of *Bsx* mutant mice indicates that *Npy* and *Agrp* expression as well as hypothalamic control of locomotory behavior depends on Bsx function. Mice deficient for Bsx lose 50% of their spontaneous physical activity and fail to increase home cage activity upon food deprivation. That locomotory behavior and body weight control might rely on overlapping hypothalamic neuronal networks is supported by analysis of other mouse mutants.

For example, Leptin-deficient mice also have decreased locomotor activity. However, rescue of leptin signaling in mice deficient for leptin or the leptin receptor normalizes their locomotor activity before any benefits in terms of weight reduction can be observed, pointing toward a body weight-independent neuroendocrine control of spontaneous physical activity (Coppari et al., 2005; Pelleymounter et al., 1995). The existence of an as yet unknown hypothalamic control of locomotor acitivity would be consistent with the observation that caloric restriction leads to an immediate change in locomotory behavior of rodents. An essential requirement for Bsx function in locomotory behavior control is further supported by the $Bsx^{\Delta HD/\Delta HD}$;*ob*/*ob* phenotype, where locomotor activity of *ob*/*ob* mice was not increased despite a significant reduction in body weight. Furthermore, it is well established that loss of MCH improves locomotor activity in *ob*/*ob* mice, and that this reduces their obesity syndrome (Segal-Lieberman et al., 2003a). In addition, disruption of the MCH receptor 1 has been reported to lead to hyperactivity (Marsh et al., 2002). Interestingly, NPY/AgRP neurons have projections to MCH-expressing neurons in the LHA (Elias et al., 1999). Consequently, NPY/AgRP neurons may modulate the dopaminergic system through MCH-expressing neurons; this circuit would represent a major component within the CNS network that regulates locomotory behavior (Zhou and Palmiter, 1995).

Although we favor the interpretation that the main locomotory behavior phenotype in *Bsx* mutant mice originates in the NPY/AgRP neurons (Coppari et al., 2005) there are two other *Bsx*-expressing neuronal populations located in the DMH and LHA of the hypothalamus that could contribute to the locomotory behavior phenotype of *Bsx* mutant mice. In particular, lesion studies of the DMH have demonstrated an involvement of this region in food-entrainable circadian rhythms (Gooley et al., 2006). However, it is hard to address if Bsx-positive neurons in the DMH are required for circadian food entrainable rhythms due to the low amplitude of locomotor activity seen in *Bsx* mutant mice. Similarly, a small population of Bsx-expressing neurons in the LHA is directly intermingled with MCH- and Orexin-expressing neurons and may directly influence these neuronal populations (Figures S1J and S1K). Thus, the individual contribution of each of these Bsx-positive

(J) Chromatin immunoprecipitation using a Bsx specific antibody shows occupancy of Bsx on the predicted binding site in isolated H2BeGFP labeled hypothalamic cells from heterozygous but not *Bsx* mutant mice.
(K) GST pull-down interaction assay with GST::Bsx and in vitro translated full length FoxO1 protein and GST::FoxO1 with in vitro translated Bsx protein.
(L) Model of *Agrp* gene regulation.

populations to the observed locomotory behavior phenotype in *Bsx* mutant mice awaits genetic dissection. Recent studies have suggested that wide differences in spontaneous physical activity observed in humans may be biologically rather than environmentally determined (Levine et al., 2005; Wilkin et al., 2006). The current data support the hypothesis that Bsx activity is one important molecular determinant of calorically relevant locomotory behavior.

Future studies on the regulation of Bsx activity and the transcriptional network underlying NPY/AgRP physiology may provide new insight into the mechanisms that are responsible both for adaptive hyperphagia as well as spontaneous physical activity and might open new avenues to control obesity. Finally, the homeobox in Bsx is highly conserved among *Drosophila*, C.elegans, fish and mammals (Jones and McGinnis, 1993). This raises the possibility that Bsx might be part of an evolutionarily conserved system to control food acquisition and body weight regulation.

EXPERIMENTAL PROCEDURES

Animals

Mice were housed in specific pathogen-free, light (12 hr light/dark cycle), temperature- (23°C) and humidity- (50%–60% relative humidity) controlled conditions. Animals were fed with regular chow diet (Harlan Winkelmann, Teklad, TD2018S); food and water were always freely available except where otherwise indicated. The procedures for performing animal experiments were in accordance with the principles and guidelines of the LAR/EMBL. The $Bsx^{\Delta HD}$ allele was backcrossed for at least 10 generations to C57/BL6J before the physiological measurements and interbreeding with *ob* mice were performed. The $Bsx^{H2beGFP}$ allele is on a mixed 129Sv/C57BL6J background. Mice carrying the *ob* mutation were obtained from Jackson Laboratories (ME, USA).

Generation of *Bsx* Alleles

$Bsx^{\Delta HD}$ and $Bsx^{H2beGFP}$ alleles were generated using standard mouse embryonic stem cell technology using R1 ES cells. 129 BAC was isolated and an 8 kb BamHI-fragment was subcloned containing the *Bsx* genomic locus. Detailed description and genotyping strategy can be found in Supplemental Experimental Procedures.

Combined In Situ Hybridization Immunohistochemistry

Anesthetized animals were transcardially perfused with 10% formalin; the brains were removed and postfixed over night at 4°C with 10% formalin. Hybridization with ^{35}S-UTP labeled (GE/Amersham Bioscience) antisense RNA probes was performed on 18 μm cryosections as previously described (Treier et al., 1998). Images were captured by using a Leica DC 500 camera attached to a Zeiss axiophot compound microscope.

For the fluorescent in situ hybridization, antisense RNA probes were labeled with digoxigenin-UTP (Roche Diagnostics) according to the manufacturer's protocol. Immunological detection of digoxigenin-labeled probes was performed according to manufacturer's protocol (Roche Diagnostics). Immunological detection of GFP was performed with a primary rabbit antibody against GFP (1:400 dilution, Torey Pines) incubated simultaneously with the anti-digoxigenin antibody. After color development with FastRed tablets (Roche Diagnostics), the reaction was stopped and the sections were incubated with a secondary FITC coupled antibody (1:400 dilution, Molecular Probes) for 1 hr at RT. Sections were next washed 3 times in PBS containing 1%Triton-X and mounted with Mowiol for microscopy. Images were captured by using a Leica TCS SP2 confocal Laser scanning microscope.

Measurement of Neuropeptide mRNA Levels

Bsx mutant and littermate controls were euthanized by cervical dislocation, and RNA was extracted from hypothalamic wedges using Qiagen RNAeasy kit.

Relative mRNA expression was determined by quantitative RT-PCR on an ABI Applied Biosystems 7500 instrument using ABI SYBR green PCR master mix. Data analysis was done using relative expression software tool, REST (Pfaffl et al., 2002) using *Gapdh* and *β-actin* as the reference genes. Oligonucleotide primer sequences can be found in Supplemental Experimental Procedures.

Immunohistochemistry

Anesthetized mice were perfused transcardially with PBS containing 2% paraformaldehyde. The brains were removed and postfixed over night in 2% paraformaldehyde. For double immunohistochemistry, free-floating 50 μm vibrotome sections were used (Leica VT1000S). Sections were next incubated in blocking solution (PBS containing 0.4% Triton-X, 5% serum corresponding to the secondary antibody) for 1 hr at room temperature followed by over night incubation with the primary antibodies at 4°C. The sections were washed the next day (0.4% Triton-X in PBS) and incubated for 1 hr at room temperature with the secondary antibodies. Bsx was detected with two antibodies we generated, an antibody raised in rabbit, immunized and boosted with the full-length protein Bsx and diluted 1:200, and a second specific antibody raised in rat immunized and boosted with a truncated form of Bsx containing only the Carboxy terminus of the protein diluted 1:100. NPY was detected with a rabbit anti-NPY (1:200 dilution, Peninsula Laboratories Inc, Bachem), AgRP with a rabbit anti-AgRP (1:200 dilution, Alpha Diagnostic international), β-endorphin with a rabbit anti-βendorphin (1:500 dilution, Parlow), α-MSH with a sheep anti-α-MSH (1:5000, Chemicon International), and Fos with a rabbit anti-Fos (1:500, Oncogene Research products). The secondary antibodies used were: Cy3-labeled anti-rabbit Immunoglobin G (IgG), Cy3-labeled anti-rat IgG, FITC-labeled anti-sheep, Cy2-labeled anti-rabbit IgG, Cy3-labeled anti chicken IgG (all by Jackson ImmunoResearch raised in Donkey).

Colchicine Administration

For the colocalization immunohistochemistry performed for Bsx and the hypothalamic neuropeptides, wild-type mice were treated with Colchicine (Sigma) in order to enhance cell-body staining 24 hr before the perfusion. 60 μg Colchicine (10 mg/ml in 0.9% saline) has been administrated in the third ventricle of the mice, by usage of a stereotaxical table.

Physiological Measurements

Body Composition

Body fat mass was measured in all mice on day 75 of age in duplicates using Nuclear Magnetic Resonance (QMR, EchoMRI, Quantitative Magnetic Resonance Body Composition Analyzer, Echo Medical Systems, Houston, TX, USA [Taicher et al., 2003; Tinsley et al., 2004]), which allows repeated measurements in conscious animals. Lean mass was calculated by subtracting fat mass from body weight measured prior to NMR measurement.

Locomotor Activity

Gross locomotor activity of mice was measured using biotelemtry (Mini Mitter Co., Inc., Bend, OR, USA). This system requires implantation of transponders into the abdominal cavity and the mouse cage to be placed on a receiver. The current location of the transponder signal on the receiver area compared to the previous measurement is interpreted as movement. Localization of the transponder signal on the receiver was measured every 5 min. A second technique for the measurement of mouse locomotor activity within home cage environment was based on number of breaks of an infrared light beam system (TSE, Bad Homburg) and was used for confirmation of principal findings as well as for the quantification of fasting induced stimulation of locomotor activity.

Energy Expenditure

Energy expenditure was measured by indirect calorimetry using a self-constructed system equipped with the gas analyzing system Advance Optima from ABB AG (Mannheim, Germany, formerly Hartmann & Braun). The system provides one measurement every 6 min per cage. Energy expenditure of mice was evaluated at the age of 8–12 weeks. Mice were adapted to respiratory cages for 2 days. Adaptation was followed by a 2 day measurement period. Before and after the measurement period, mice were analyzed for body composition using Nuclear Magnetic Resonance imaging for calculation of lean mass-specific energy expenditure.

GST Pull-Down Assay

In brief, after purification with glutathione sepharose beads, GST and GST fusion proteins were loaded on an SDS-acrylamide gel for quantification. 2 μg of protein coupled with the matrix were used in each sample. The full-length mouse Bsx, CREB, and FoxO1 proteins were expressed and purified as GST fusions proteins in the pET-41a-c bacteria vector (Novagen). GST::Bsx, GST::CREB and GST::FoxO1 were added to the standard GST pull-down with in vitro translated CREB, full length Bsx or FoxO1 labeled with Methionine-^{35}S (in vitro translation kit: TNT coupled reticulocyte lysate systems, Promega, Methionine-^{35}S from Amersham). The reaction was allowed to proceed for 2 hr at 4°C in PBS 0.1% Tween w/w. Samples were next washed 5 times with PBS containing 0.5% Tween w/w and loaded on a SDS-acrylamide gel. The data were then analyzed by autoradiography.

Cell Culture-qRT-PCR Analysis

AtT20 cells and PC-12 cells were obtained from ATCC and transfected with lipofectamin 2000 (Invitrogen). Cells were treated with Phorbol-12-myristate-13-acetate (PMA, Sigma) and 2′-0-Dibutryladenosine-3′,5′-cyclic-monophosphate sodium salt (DibcAMP, Sigma) as indicated. QRT-PCR was performed to quantify *Npy* and *Agrp* mRNA isolated from PC-12 and AtT20 cells, respectively. Primers are listed in Supplemental Experimental Procedures.

ChIP Assays

"Carrier" ChIP assay was performed on 25,000 FACS sorted GFP-positives neurons from 12 $Bsx^{H2BeGFP/+}$ and 12 $Bsx^{H2BeGFP/DHD}$ mice (O'Neill et al., 2006). GFP-positive neurons were sorted on a modified Dako MoFlo sorter (DAKO GmbH, Hamburg Germany D-22083). The primers used for *Agrp*: 5′-CGGAAGGGAGCAGCCAT-3′ (forward) and 5′-TCCTGGCTCTCCCTCCT-3′ (reverse) (−676 to −479) and control: 5′-GCAGACAGCATCCAG-3′ (forward) and 5′-CGATGGAACATC CAGT-3′ (reverse) (−11.3 to −11.4 kb). For *Npy*: 5′-GCAGCCTTCA TATCG-3′ (forward) and 5′-GCTCTGTGATGTTC-3′ (reverse) (−48.5 to −48.3 kb) and control: 5′-GCATGGCTCACCAT-3′ (forward) and 5′-CCAGCCAGCCCAGTA-3′ (reverse) (−59.9 to −59.7 kb). The rabbit antibody against Bsx was used for the IP and the rabbit antibody against GFP was used for the mock control IP.

Luciferase Assays

AtT20 or PC12 cells were transfected with luciferase reporter constructs containing the *Agrp* promoter (nucleotides −700 to −1) or the *Npy cis*-regulatory modules (−48,823 to −48,174) along with control, Bsx and/or FoxO1-ADA expression vectors. Renilla plasmid (Promega) was cotransfected as control for transfection efficiency. Cells were treated with Phorbol-12-myristate-13-acetate (PMA, Sigma) and 2′-O-Dibutyryladenosine-3′, 5′-cyclic-monophosphate sodium salt (Dibc AMP, Sigma) as indicated. Luciferase activity was determined using the Dual-Luciferase Reporter Assay kit (Promega).

Statistical Analyses

Data are presented as means ± SEM. All data were normally distributed. Two-sample t test was applied to calculate significance between the fat mass of $Bsx^{\Delta HD/\Delta HD}$ and the control wild-type. Analysis of variance was calculated by applying Kruskal-Wallis tests (for the refeeding and locomotion measurements during the fasting experiment, for the real-time PCR data, the fat mass, food intake, and body temperature measurements of the double-mutant $Bsx^{\Delta HD/\Delta HD}$ *ob/ob* mice, and the endocrine parameters measurements). The test was followed by Tukey's post hoc tests (for the real-time PCR data, the fat mass, food intake, and body temperature measurements of the double-mutant $Bsx^{\Delta HD/\Delta HD}$ *ob/ob* mice, and the endocrine parameters measurements). For all analyses, significance was assigned at the $p < 0.05$ level.

Supplemental Data

Supplemental Data include Supplemental Experimental Procedures, Supplemental References, five figures, and one table and can be found with this article online at http://www.cellmetabolism.org/cgi/content/full/5/6/450/DC1/.

ACKNOWLEDGMENTS

We want to thank Christopher B. Kaelin and Gregory S. Barsh for sharing data prior to publication. Carola Plaue for expert technical assistance; Domenic Accili for FoxO1 expression vectors; Roberto DiLauro for the Nkx2.1/TTF-1 expression vector; Günther Schütz for CREB cDNAs; Kat Hadjantonakis for the Histone2bEGFP construct; A.F. Parlow and the National Hormone and Peptide Program (NHPP) for reagents; Stephen C. Woods and Randy J. Seeley for critical reading of the manuscript; and the staff of the EMBL Laboratory Animal Resources for expert animal support. This work was supported in part by grant EU FP6 funding (DIABESITY contract LSHM-CT-503041, M.T. and M.H.T., and 1RO1DK069987-01 and P01DK056863, M.H.T.).

Received: January 29, 2007
Revised: April 12, 2007
Accepted: May 14, 2007
Published: June 5, 2007

REFERENCES

Badman, M.K., and Flier, J.S. (2005). The gut and energy balance: visceral allies in the obesity wars. Science *307*, 1909–1914.

Barsh, G.S., and Schwartz, M.W. (2002). Genetic approaches to studying energy balance: perception and integration. Nat. Rev. Genet. *3*, 589–600.

Bates, S.H., Stearns, W.H., Dundon, T.A., Schubert, M., Tso, A.W., Wang, Y., Banks, A.S., Lavery, H.J., Haq, A.K., Maratos-Flier, E., et al. (2003). STAT3 signalling is required for leptin regulation of energy balance but not reproduction. Nature *421*, 856–859.

Castaneda, T.R., Jurgens, H., Wiedmer, P., Pfluger, P., Diano, S., Horvath, T.L., Tang-Christensen, M., and Tschop, M.H. (2005). Obesity and the neuroendocrine control of energy homeostasis: the role of spontaneous locomotor activity. J. Nutr. *135*, 1314–1319.

Chen, H.Y., Trumbauer, M.E., Chen, A.S., Weingarth, D.T., Adams, J.R., Frazier, E.G., Shen, Z., Marsh, D.J., Feighner, S.D., Guan, X.M., et al. (2004). Orexigenic action of peripheral ghrelin is mediated by neuropeptide Y and agouti-related protein. Endocrinology *145*, 2607–2612.

Cone, R.D. (2005). Anatomy and regulation of the central melanocortin system. Nat. Neurosci. *8*, 571–578.

Coppari, R., Ichinose, M., Lee, C.E., Pullen, A.E., Kenny, C.D., McGovern, R.A., Tang, V., Liu, S.M., Ludwig, T., Chua, S.C., Jr., et al. (2005). The hypothalamic arcuate nucleus: a key site for mediating leptin's effects on glucose homeostasis and locomotor activity. Cell Metab. *1*, 63–72.

Cowley, M.A., Smith, R.G., Diano, S., Tschop, M., Pronchuk, N., Grove, K.L., Strasburger, C.J., Bidlingmaier, M., Esterman, M., Heiman, M.L., et al. (2003). The distribution and mechanism of action of ghrelin in the CNS demonstrates a novel hypothalamic circuit regulating energy homeostasis. Neuron *37*, 649–661.

Cremona, M., Colombo, E., Andreazzoli, M., Cossu, G., and Broccoli, V. (2004). Bsx, an evolutionary conserved Brain Specific homeoboX gene expressed in the septum, epiphysis, mammillary bodies and arcuate nucleus. Gene Expr. Patterns *4*, 47–51.

Elias, C.F., Aschkenasi, C., Lee, C., Kelly, J., Ahima, R.S., Bjorbaek, C., Flier, J.S., Saper, C.B., and Elmquist, J.K. (1999). Leptin differentially regulates NPY and POMC neurons projecting to the lateral hypothalamic area. Neuron *23*, 775–786.

Elias, C.F., Saper, C.B., Maratos-Flier, E., Tritos, N.A., Lee, C., Kelly, J., Tatro, J.B., Hoffman, G.E., Ollmann, M.M., Barsh, G.S., et al. (1998). Chemically defined projections linking the mediobasal hypothalamus and the lateral hypothalamic area. J. Comp. Neurol. *402*, 442–459.

Erickson, J.C., Clegg, K.E., and Palmiter, R.D. (1996a). Sensitivity to leptin and susceptibility to seizures of mice lacking neuropeptide Y. Nature *381*, 415–421.

Erickson, J.C., Hollopeter, G., and Palmiter, R.D. (1996b). Attenuation of the obesity syndrome of ob/ob mice by the loss of neuropeptide Y. Science *274*, 1704–1707.

Farooqi, I.S., and O'Rahilly, S. (2005). Monogenic obesity in humans. Annu. Rev. Med. *56*, 443–458.

Flier, J.S. (2004). Obesity wars: molecular progress confronts an expanding epidemic. Cell *116*, 337–350.

Friedman, J.M. (2004). Modern science versus the stigma of obesity. Nat. Med. *10*, 563–569.

Friedman, J.M., and Halaas, J.L. (1998). Leptin and the regulation of body weight in mammals. Nature *395*, 763–770.

Georgescu, D., Sears, R.M., Hommel, J.D., Barrot, M., Bolanos, C.A., Marsh, D.J., Bednarek, M.A., Bibb, J.A., Maratos-Flier, E., Nestler, E.J., and DiLeone, R.J. (2005). The hypothalamic neuropeptide melanin-concentrating hormone acts in the nucleus accumbens to modulate feeding behavior and forced-swim performance. J. Neurosci. *25*, 2933–2940.

Gooley, J.J., Schomer, A., and Saper, C.B. (2006). The dorsomedial hypothalamic nucleus is critical for the expression of food-entrainable circadian rhythms. Nat. Neurosci. *9*, 398–407.

Gropp, E., Shanabrough, M., Borok, E., Xu, A.W., Janoschek, R., Buch, T., Plum, L., Balthasar, N., Hampel, B., Waisman, A., et al. (2005). Agouti-related peptide-expressing neurons are mandatory for feeding. Nat. Neurosci. *8*, 1289–1291.

Hagan, M.M., Rushing, P.A., Pritchard, L.M., Schwartz, M.W., Strack, A.M., Van Der Ploeg, L.H., Woods, S.C., and Seeley, R.J. (2000). Long-term orexigenic effects of AgRP-(83—132) involve mechanisms other than melanocortin receptor blockade. Am. J. Physiol. Regul. Integr. Comp. Physiol. *279*, R47–R52.

Hahn, T.M., Breininger, J.F., Baskin, D.G., and Schwartz, M.W. (1998). Coexpression of Agrp and NPY in fasting-activated hypothalamic neurons. Nat. Neurosci. *1*, 271–272.

Hewson, A.K., and Dickson, S.L. (2000). Systemic administration of ghrelin induces Fos and Egr-1 proteins in the hypothalamic arcuate nucleus of fasted and fed rats. J. Neuroendocrinol. *12*, 1047–1049.

Higuchi, H., Yang, H.Y., and Sabol, S.L. (1988). Rat neuropeptide Y precursor gene expression. mRNA structure, tissue distribution, and regulation by glucocorticoids, cyclic AMP, and phorbol ester. J. Biol. Chem. *263*, 6288–6295.

Huszar, D., Lynch, C.A., Fairchild-Huntress, V., Dunmore, J.H., Fang, Q., Berkemeier, L.R., Gu, W., Kesterson, R.A., Boston, B.A., Cone, R.D., et al. (1997). Targeted disruption of the melanocortin-4 receptor results in obesity in mice. Cell *88*, 131–141.

Jones, B., and McGinnis, W. (1993). A new Drosophila homeobox gene, bsh, is expressed in a subset of brain cells during embryogenesis. Development *117*, 793–806.

Kaelin, C.B., Gong, L., Xu, A.W., Yao, F., Hockman, K., Morton, G.J., Schwartz, M.W., Barsh, G.S., and MacKenzie, R.G. (2006). Signal transducer and activator of transcription (stat) binding sites but not stat3 are required for fasting-induced transcription of agouti-related protein messenger ribonucleic acid. Mol. Endocrinol. *20*, 2591–2602.

Kesterson, R.A., Huszar, D., Lynch, C.A., Simerly, R.B., and Cone, R.D. (1997). Induction of neuropeptide Y gene expression in the dorsal medial hypothalamic nucleus in two models of the agouti obesity syndrome. Mol. Endocrinol. *11*, 630–637.

Kitamura, T., Feng, Y., Kitamura, Y.I., Chua, S.C., Jr., Xu, A.W., Barsh, G.S., Rossetti, L., and Accili, D. (2006). Forkhead protein FoxO1 mediates Agrp-dependent effects of leptin on food intake. Nat. Med. *12*, 534–540.

Lee, Y.S., Challis, B.G., Thompson, D.A., Yeo, G.S., Keogh, J.M., Madonna, M.E., Wraight, V., Sims, M., Vatin, V., Meyre, D., et al. (2006). A POMC variant implicates beta-melanocyte-stimulating hormone in the control of human energy balance. Cell Metab. *3*, 135–140.

Levine, J.A., Lanningham-Foster, L.M., McCrady, S.K., Krizan, A.C., Olson, L.R., Kane, P.H., Jensen, M.D., and Clark, M.M. (2005). Interindividual variation in posture allocation: possible role in human obesity. Science *307*, 584–586.

Luquet, S., Perez, F.A., Hnasko, T.S., and Palmiter, R.D. (2005). NPY/AgRP neurons are essential for feeding in adult mice but can be ablated in neonates. Science *310*, 683–685.

Marsh, D.J., Weingarth, D.T., Novi, D.E., Chen, H.Y., Trumbauer, M.E., Chen, A.S., Guan, X.M., Jiang, M.M., Feng, Y., Camacho, R.E., et al. (2002). Melanin-concentrating hormone 1 receptor-deficient mice are lean, hyperactive, and hyperphagic and have altered metabolism. Proc. Natl. Acad. Sci. USA *99*, 3240–3245.

Morrison, C.D., Morton, G.J., Niswender, K.D., Gelling, R.W., and Schwartz, M.W. (2005). Leptin inhibits hypothalamic Npy and Agrp gene expression via a mechanism that requires phosphatidylinositol 3-OH-kinase signaling. Am. J. Physiol. Endocrinol. Metab. *289*, E1051–E1057.

Morton, G.J., Cummings, D.E., Baskin, D.G., Barsh, G.S., and Schwartz, M.W. (2006). Central nervous system control of food intake and body weight. Nature *443*, 289–295.

O'Neill, L.P., VerMilyea, M.D., and Turner, B.M. (2006). Epigenetic characterization of the early embryo with a chromatin immunoprecipitation protocol applicable to small cell populations. Nat. Genet. *38*, 835–841.

Overton, J.M., and Williams, T.D. (2004). Behavioral and physiologic responses to caloric restriction in mice. Physiol. Behav. *81*, 749–754.

Pelleymounter, M.A., Cullen, M.J., Baker, M.B., Hecht, R., Winters, D., Boone, T., and Collins, F. (1995). Effects of the obese gene product on body weight regulation in ob/ob mice. Science *269*, 540–543.

Pfaffl, M.W., Horgan, G.W., and Dempfle, L. (2002). Relative expression software tool (REST) for group-wise comparison and statistical analysis of relative expression results in real-time PCR. Nucleic Acids Res. *30*, e36.

Qian, S., Chen, H., Weingarth, D., Trumbauer, M.E., Novi, D.E., Guan, X., Yu, H., Shen, Z., Feng, Y., Frazier, E., et al. (2002). Neither agouti-related protein nor neuropeptide Y is critically required for the regulation of energy homeostasis in mice. Mol. Cell. Biol. *22*, 5027–5035.

Schwartz, M.W., and Porte, D., Jr. (2005). Diabetes, obesity, and the brain. Science *307*, 375–379.

Scully, K.M., and Rosenfeld, M.G. (2002). Pituitary development: regulatory codes in mammalian organogenesis. Science *295*, 2231–2235.

Segal-Lieberman, G., Bradley, R.L., Kokkotou, E., Carlson, M., Trombly, D.J., Wang, X., Bates, S., Myers, M.G., Jr., Flier, J.S., and Maratos-Flier, E. (2003a). Melanin-concentrating hormone is a critical mediator of the leptin-deficient phenotype. Proc. Natl. Acad. Sci. USA *100*, 10085–10090.

Segal-Lieberman, G., Trombly, D.J., Juthani, V., Wang, X., and Maratos-Flier, E. (2003b). NPY ablation in C57BL/6 mice leads to mild obesity and to an impaired refeeding response to fasting. Am. J. Physiol. Endocrinol. Metab. *284*, E1131–E1139.

Shimizu-Albergine, M., Ippolito, D.L., and Beavo, J.A. (2001). Downregulation of fasting-induced cAMP response element-mediated gene induction by leptin in neuropeptide Y neurons of the arcuate nucleus. J. Neurosci. *21*, 1238–1246.

Sindelar, D.K., Palmiter, R.D., Woods, S.C., and Schwartz, M.W. (2005). Attenuated feeding responses to circadian and palatability cues in mice lacking neuropeptide Y. Peptides *26*, 2597–2602.

Taicher, G.Z., Tinsley, F.C., Reiderman, A., and Heiman, M.L. (2003). Quantitative magnetic resonance (QMR) method for bone and whole-body-composition analysis. Anal. Bioanal. Chem. *377*, 990–1002.

Thorpe, A.J., and Kotz, C.M. (2005). Orexin A in the nucleus accumbens stimulates feeding and locomotor activity. Brain Res. *1050*, 156–162.

Tinsley, F.C., Taicher, G.Z., and Heiman, M.L. (2004). Evaluation of a quantitative magnetic resonance method for mouse whole body composition analysis. Obes. Res. *12*, 150–160.

Tou, J.C., and Wade, C.E. (2002). Determinants affecting physical activity levels in animal models. Exp. Biol. Med. (Maywood) *227*, 587–600.

Treier, M., Gleiberman, A.S., O'Connell, S.M., Szeto, D.P., McMahon, J.A., McMahon, A.P., and Rosenfeld, M.G. (1998). Multistep signaling requirements for pituitary organogenesis in vivo. Genes Dev. *12*, 1691–1704.

Tschop, M., Smiley, D.L., and Heiman, M.L. (2000). Ghrelin induces adiposity in rodents. Nature *407*, 908–913.

Wilkin, T.J., Mallam, K.M., Metcalf, B.S., Jeffery, A.N., and Voss, L.D. (2006). Variation in physical activity lies with the child, not his environment: evidence for an 'activitystat' in young children (EarlyBird 16). Int. J. Obes. (London) *30*, 1050–1055.

Williams, T.D., Chambers, J.B., Roberts, L.M., Henderson, R.P., and Overton, J.M. (2003). Diet-induced obesity and cardiovascular regulation in C57BL/6J mice. Clin. Exp. Pharmacol. Physiol. *30*, 769–778.

Woods, S.C., Seeley, R.J., Porte, D., Jr., and Schwartz, M.W. (1998). Signals that regulate food intake and energy homeostasis. Science *280*, 1378–1383.

Wortley, K.E., Anderson, K.D., Yasenchak, J., Murphy, A., Valenzuela, D., Diano, S., Yancopoulos, G.D., Wiegand, S.J., and Sleeman, M.W. (2005). Agouti-related protein-deficient mice display an age-related lean phenotype. Cell Metab. *2*, 421–427.

Xu, A.W., Kaelin, C.B., Takeda, K., Akira, S., Schwartz, M.W., and Barsh, G.S. (2005). PI3K integrates the action of insulin and leptin on hypothalamic neurons. J. Clin. Invest. *115*, 951–958.

Zhou, Q.Y., and Palmiter, R.D. (1995). Dopamine-deficient mice are severely hypoactive, adipsic, and aphagic. Cell *83*, 1197–1209.